Bioorganic & Medicinal Chemistry Letters 23 (2013) 1398–1406

Contents lists available at SciVerse ScienceDirect

Bioorganic & Medicinal Chemistry Letters

journal homepage: www.elsevier.com/locate/bmcl

Discovery and structure–activity relationship of 1,3-cyclohexyl amide derivatives as novel mGluR5 negative allosteric modulators

Hao Zhou [a], Sidney W. Topiol [a,†], Michel Grenon [a], Hermogenes N. Jimenez [a], Michelle A. Uberti [b], Daniel G. Smith [b], Robbin M. Brodbeck [b], Gamini Chandrasena [c], Henrik Pedersen [d], Jens Christian Madsen [d,‡], Darío Doller [a], Guiying Li [a,*]

[a] Discovery Chemistry & DMPK, Lundbeck Research USA, 215 College Road, Paramus, NJ 07652, USA
[b] Molecular Pharmacology & SAR, Lundbeck Research USA, 215 College Road, Paramus, NJ 07652, USA
[c] Bioanalysis & Physiology, Lundbeck Research USA, 215 College Road, Paramus, NJ 07652, USA
[d] Discovery Chemistry & DMPK, H. Lundbeck A/S, Ottiliavej 9, DK-2500 Valby, Denmark

ARTICLE INFO

Article history:
Received 9 November 2012
Revised 17 December 2012
Accepted 21 December 2012
Available online 5 January 2013

Keywords:
mGluR5
Negative allosteric modulator

ABSTRACT

A novel series of *trans*-1,3-cyclohexyl diamides was discovered and characterized as mGluR5 negative allosteric modulators (NAMs) lacking an alkyne moiety. Conformational constraint of one of the amide bonds in the diamide template led to a spirooxazoline template. A representative compound (**24d**) showed good in vitro potency, high CNS penetration and, upon subcutaneous dosing, demonstrated efficacy in the mouse marble burying test, generally used as indicative of potential anxiolytic activity.

Glutamic acid is the major excitatory neurotransmitter in the central nervous system (CNS) and exerts its signaling function by activating ionotropic (iGluRs) and metabotropic glutamate receptors (mGluRs). iGluRs are ligand-gated ion channels that mediate fast excitatory transmission in many physiological functions, and have been divided into three classes based on their selective interactions with different ligands: α-amino-3-hydroxy-5-methyl-4-isoxazole propionic acid (AMPA), kainic acid (KA), and *N*-methyl-D-aspartic acid (NMDA).[1,2] The mGluRs belong to the class C of G-protein coupled receptor (GPCR) superfamily and mediate slower neurotransmission.[3] Eight different mGluR subtypes have been identified and divided into group I (mGluR1 and 5), group II (mGluR2 and 3), and group III (mGluR4, 6, 7 and 8) based on sequence homology, second messenger coupling and pharmacology.[4] mGluR5s are mostly localized postsynaptically, couple to $G_{q/11}$ proteins and activate phospholipase C, leading to phosphoinositide hydrolysis and formation of two intracellular second messengers: inositol triphosphate (IP3), which induces intracellular Ca^{2+} release, and diacylglycerol (DAG), which can activate protein kinase C.[5,6] Orthosteric ligands of mGluRs bind in the extracellular amino-terminal domain. Some recent design strategies have succeeded in delivering highly selective orthosteric mGluR ligands.[7] However, in general, these suffer from poor selectivity within mGluR subtypes, which is generally believed to share a relatively highly conserved binding region, although this hypothesis has recently been challanged.[8] Allosteric binding sites exist in the receptor cell transmembrane domain, which is housed by what is believed to be the less-conserved amino acids than at the orthosteric site of the receptors. Thus, the strategy of designing ligands targeting this region has often produced selective receptor modulation.[9] mGluR5 negative allosteric modulators have been actively pursued as a potential treatment for anxiety, depression, pain, levodopa-induced dyskinesia in Parkinson's disease (LID-PD), gastroesophageal reflux disease (GERD), cocaine addiction and Fragile X Syndrome (FXS).[10–12] Some of these indications already have Phase II clinical proof of concept, including FXS,[13] LID-PD,[14] GERD,[15] and anxiety.[16] Currently, there are a number of mGluR5 NAMs in the clinic, including Novartis' AFQ056 (**1**, Phase II/III for FXS and LID-PD), Roche's RO4917523 (**2**, Phase II for FXS and treatment-resistant depression (TRD)), Addex's ADX48621 (**3**, Phase II for LID-PD) and Seaside's STX107 (**4**, Phase I for FXS). Similar to MPEP (**5**), these compounds contain an alkyne moiety as a key structural component. Recent chemistry work has focused on exploring non-alkyne chemotypes, in particular after termination of the development of Addex's first generation alkyne-containing mGluR5 NAM, ADX10059 (**6**), due to observed liver function abnormalities in the clinical studies.[17] These efforts yielded a number of mGluR5 NAMs free from alkyne functionalitites, such

* Corresponding author. Tel.: +201 350 0140.
E-mail address: guli@lundbeck.com (G. Li).
† Present address: 3D-2drug, PO Box 184, Fair Lawn, NJ 07410, USA.
‡ Present address: Bruker Biospin Scandinavia AB, Vallgatan 5, SE-17067 Solna, Sweden.

0960-894X/$ - see front matter © 2012 Elsevier Ltd. All rights reserved.
http://dx.doi.org/10.1016/j.bmcl.2012.12.078

as compounds **7**–**12** (see Fig. 1).[18a–f] Progress in non-alkyne chemical space has been summarized in a recent review.[18g] Herein we report the rational design, synthesis, and structure–activity relationships (SAR) of 1,3-cyclohexyl amide derivatives as a novel series of mGluR5 NAMs lacking an alkyne moiety.

In search for novel allosteric mGluR5 chemical space, a computational overlay model was built reflecting a simple binding hypothesis.[19] It was observed that two literature compounds **13**[20a] and **14**[20b] (Fig. 2) with different multi-ring systems had similar (hetero)aryl rings at both ends. We hypothesized that other compounds which would present these terminal aromatic rings in the same three-dimensional disposition, while traversing the same bridging region, would also have activity. Thus, an in silico core hopping strategy that preserved the geometric arrangement of the outer aromatic groups in compounds **13** and **14** was executed using the FlexAlign algorithm in MOE (Fig. 2).[21] A replacement was sought for the regions of **13** and **14** highlighted in green, acting as a linker to optimally position the left- and right-hand-side (hetero)aryls for binding to an mGluR5 allosteric site. The model was constructed using structures **13** and **14**, which were first overlayed using FlexAlign. These overlayed structures were then held in fixed geometries and used as the initial model. A number of possible linkers (green region in Fig. 2), such as different ring systems and/or substituents were then selected 'by hand' to create new hypothetical structures. These new structures were subjected to an overlay with the initial model to see which ones fit well with respect to the terminal aromatic rings. It was found that a cyclohexyl core with an amide (e.g., –NHCO– or –CONH–) or alkyne linker on 1- and/or 3-positions (scaffold **15**) would fit our hypothesis well, and project the outer aromatic groups in the right directions resulting in good overlaying with compounds **13** and **14**.

To test this binding hypothesis, and encouraged by the good *c*Log*P* and CNS drug-likeness multi parameter optimization (MPO[22]) values (2.7 and 5.0, respectively) of model compounds **15a** and **15b**, their preparation was undertaken using a synthetic route that expeditiously provided both the cis- and trans-isomers after preparative thin layer chromatography (TLC) separation (Scheme 1). Cis or trans stereochemical assignments were made using ^{1}H NMR and HSQC spectroscopic analysis.[23] The mGluR5 functional antagonistic activity of these compounds was evaluated in vitro measuring their ability to inhibit the calcium mobilization caused by the EC_{80} concentration of glutamate in HEK293 cells expressing human mGluR5.[24] We were delighted to find that in this assay, the trans-isomer **15a** showed an IC_{50} value of 531 nM. The cis-isomer **15b** was inactive. In addition, the allosteric nature of **15a** was supported by a displacement radioligand binding assay using [^{3}H]-ABP688,[25] where **15a** showed a K_i of 1538 nM, while **15b** was also inactive (Table 1).

These positive results encouraged us to design a small library of analogs, mostly with the active trans stereochemistry. To this end, the synthetic route was modified to stereospecifically provide either trans or cis analogs, as well as to further confirm the structural assignments. A number of compounds, including both isomers **15a** and **15b**, were prepared from the corresponding *trans*- or *cis*-3-((*tert*-butoxycarbonyl)amino)cyclohexane-carboxylic acid (**17a** and **17b**) as shown in Scheme 2. Stereospecific Curtius rearrangement with DPPA, followed by the treatment with *tert*-butyl alcohol, afforded *trans*- or *cis*-1,3-cyclohexanedi(*tert*-butoxycar-

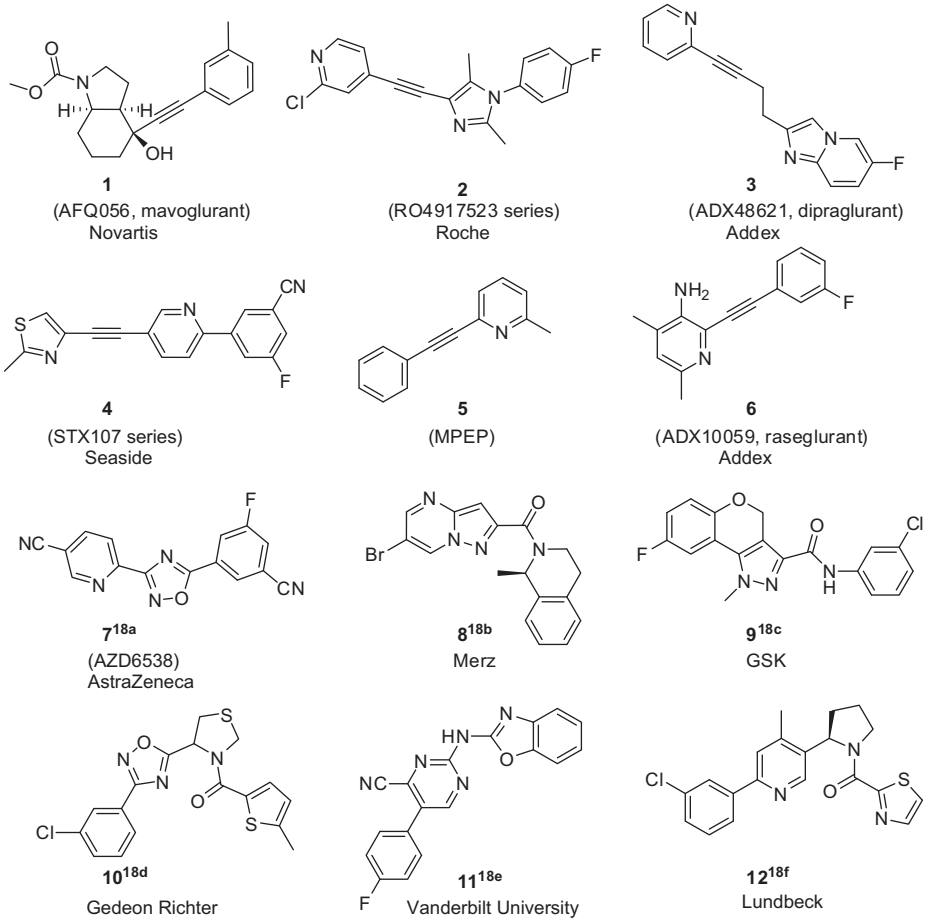

Figure 1. Structures of select mGluR5 NAMs.

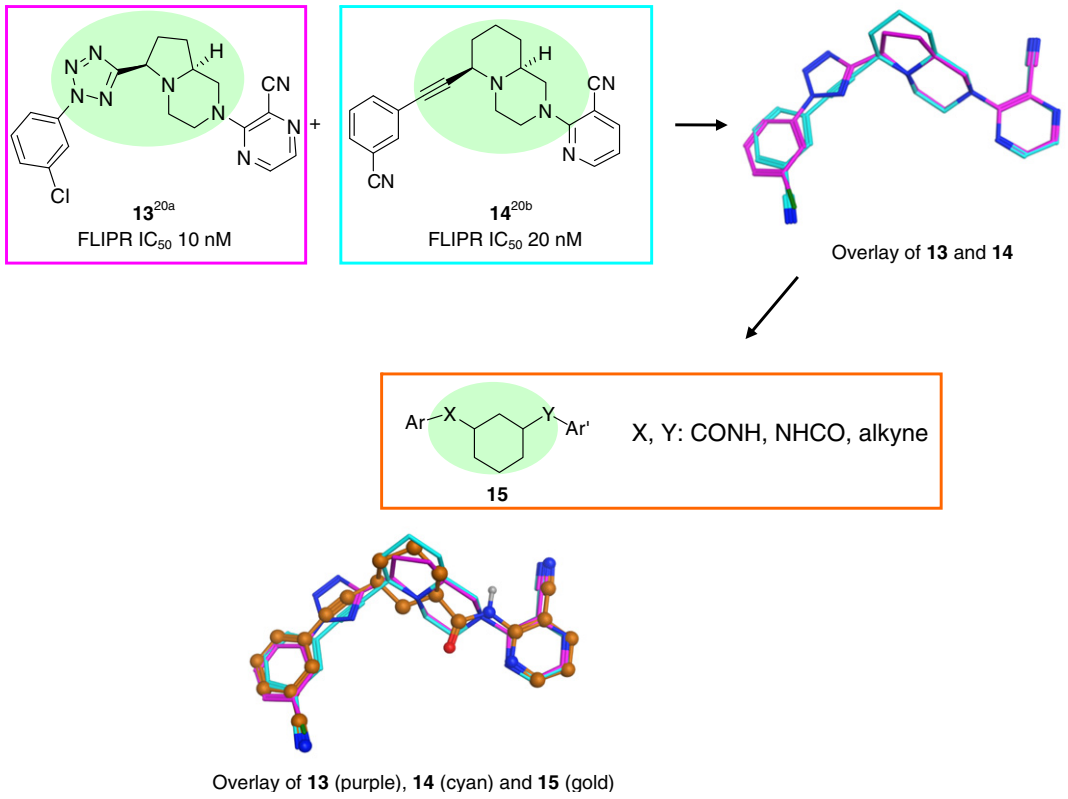

Figure 2. Overlay model.

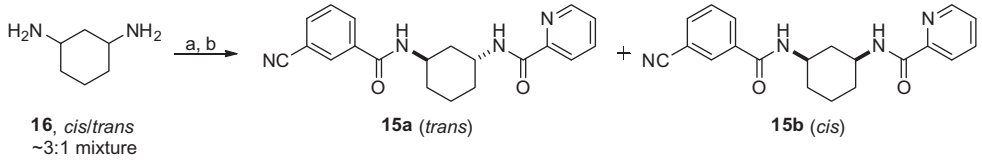

Scheme 1. Reagents and conditions: (a) (i) picolinic acid (1 equiv), BOP (1 equiv), NEt_3 (4 equiv), CH_2Cl_2, room temp, overnight, (ii) *m*-CN-$PhCO_2H$ (1 equiv), BOP (1 equiv), NEt_3 (4 equiv), CH_2Cl_2, room temp, overnight; (b) separation by preparative TLC (ethyl acetate/hexane: 1/1).

bonyl)amine (**18a** and **18b**),[26] respectively. Removal of the Boc group with TFA, followed by amidation with picolinic acid, and then amidation with 3-cyanobenzoic acid under standard conditions afforded **15a** or **15b**, respectively. Likewise, by appropriate choice of the carboxylic acid or acyl chloride, analogs **15c**–**15ag** was prepared. Table 1 shows the in vitro screening results of these compounds for mGluR5 functional activity and binding affinity, as well as select in silico properties.

Early SAR observations pointed to the 3-chlorophenyl as a preferred fragment in this core, in agreement with previous work.[18f,27] When R^2 is pyridin-2-yl, replacement of 3-cyanophenyl (**15c**) with 3-chlorophenyl (**15f**) enhanced the functional potency by 4-fold. Analogs where the 3-chlorophenyl (**15f**) is replaced with 3-anisyl (**15i**) or 3-tolyl (**15j**) were significantly less active. The mGluR5 NAM activity of symmetrically substituted diamides was briefly explored. Again, 3-chlorophenyl-bearing bis-amide **15k** was more potent than 3-fluorophenyl and pyridine-2-yl bis-amides **15l** and **15m**, respectively. At this point the decision was made to fix one side of the amide as a 3-chlorophenyl (R^1) and optimize the R^2 substituent. Among pyridyl analogs, pyridin-2-yl (**15f**) was about 2- to 5-fold more active compared to pyridin-3-yl (**15n**) and pyridin-4-yl (**15o**) in the functional assay. A methyl group on the 6-position of the pyridyl ring (**15p**) was tolerated, but on 3- or 4-position it significantly reduced the activity (**15q** and **15r**). The 3-cyano-pyridin-2-yl fragment provided ca. 11-fold more functional potency than 3-methyl-pyridin-2-yl (**15s** vs. **15r**). Phenyl (**15t**) was well tolerated. Walking the fluorine atom to positions 2, 3 or 4 in the R^2 phenyl ring did not have a significant impact on potency (**15u**, **15v** and **15y**). Electron donating methoxy group was tolerated both at 3-or 4-position (**15z** and **15aa**, respectively), while dimethylamino group was tolerated at 4-, but not at 3-position (**15ab** and **15ac**). Introduction of the second nitrogen into the pyridine ring such as in pyrimidin-2-yl amide **15ad** or pyrazin-2-yl amide **15ae** reduced functional activity by 2- and 10-fold, respectively. Aliphatic amides such as cyclohexyl (**15af**) or pyridin-2-ylmethyl (**15ag**) drastically reduced the activity.

To explore the effect of a retro-amide linker, compounds **21a**–**21c** was prepared according to Scheme 2. Reversing one of the amide bonds (i.e., –NH–CO– to –CO–NH–) has significantly negative impact on the activity (**21a** vs. **15a**, **21b** and **21c** vs. **15f**, Scheme 3). A retro-amide tether on the 3-chlorophenyl side was tolerated, but on the pyridin-2-yl side it abolished the activity.

To investigate the importance of the hydrogen donor of the -NHCO- moiety, *N*-methyl and *N,N′*-dimethyl derivatives (**22** and **23**) of symmetrically substituted **15k** were made (albeit in low yields) according to Scheme 4. These analogs were inactive in the

Table 1
In vitro mGluR5 activity and in silico properties of select 1,3-cyclohexyl diamides

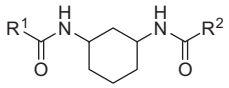

CMPD	R^1	R^2	*c*Log*P*	MPO	IC_{50}[a] (nM)	K_i[a] (nM)	LLE[b]
15a, *trans*	3-Cyanophenyl	Pyridin-2-yl	2.7	5.0	531 ± 88	1538 ± 497	3.6
15b, *cis*	3-Cyanophenyl	Pyridin-2-yl	2.7	5.0	>10,000	—	—
15c, *trans*-(*R*,*R*)[c]	3-Cyanophenyl	Pyridin-2-yl	2.7	5.0	231 ± 52	1275 ± 480	4.0
15d, *trans* (*S*,*S*)[c]	3-Cyanophenyl	Pyridin-2-yl	2.7	5.0	>10,000	—	—
15e, *cis*/*trans*[d]	3-Chlorophenyl	Pyridin-2-yl	3.7	4.3	314 ± 97	—	—
15f, *trans*-(*R*,*R*)[c]	3-Chlorophenyl	Pyridin-2-yl	3.7	4.3	62 ± 15	205 ± 46	3.5
15g, *trans*-(*S*,*S*)[c]	3-Chlorophenyl	Pyridin-2-yl	3.7	4.3	>10,000	—	1.3
15h, *cis*	3-Chlorophenyl	Pyridin-2-yl	3.7	4.3	1510 ± 110	—	2.2
15i, *cis*/*trans*[d]	3-Methoxylphenyl	Pyridin-2-yl	3.0	4.5	>10,000	—	—
15j, *trans*	3-Methylphenyl	Pyridin-2-yl	3.3	4.8	1000 ± 69	—	2.8
15k, *cis*/*trans*[d]	3-Chlorophenyl	3-Chlorophenyl	5.0	3.3	139 ± 27	—	1.9
15l, *trans*	3-Fluorophenyl	3-Fluorophenyl	3.8	4.2	593 ± 57	—	2.4
15m, *trans*	Pyridin-2-yl	Pyridin-2-yl	2.3	5.3	1150 ± 241	—	3.6
15n, *trans*	3-Chlorophenyl	Pyridin-3-yl	3.3	4.7	612 ± 92	—	2.9
15o, *trans*	3-Chlorophenyl	Pyridin-4-yl	3.3	4.7	300 ± 45	445 ± 65	3.2
15p, *trans*	3-Chlorophenyl	6-Methylpyridin-2-yl	4.2	3.8	290 ± 47	582 ± 95	2.3
15q, *trans*	3-Chlorophenyl	4-Methylpyridin-2-yl	4.2	3.8	3400 ± 410	—	1.3
15r, *trans*	3-Chlorophenyl	3-Methylpyridin-2-yl	3.8	3.8	7840 ± 354	—	1.3
15s, *cis*/*trans*[d]	3-Chlorophenyl	3-Cyanopyridin-2-yl	3.3	4.4	671 ± 102	1246 ± 125	2.9
15t, *trans*	3-Chlorophenyl	Phenyl	4.1	4.0	228 ± 28	672 ± 107	2.6
15u, *trans*	3-Chlorophenyl	2-Fluorophenyl	4.0	3.9	175 ± 6	760 ± 119	2.8
15v, *trans*	3-Chlorophenyl	3-Fluorophenyl	4.4	3.7	86 ± 20	320 ± 64	2.7
15w, *trans*-(*R*,*R*)[c]	3-Chlorophenyl	3-Fluorophenyl	4.4	3.7	59 ± 2	211 ± 62	2.8
15x, *trans*-(*S*,*S*)[c]	3-Chlorophenyl	3-Fluorophenyl	4.4	3.7	9600 ± 247	—	0.6
15y, *trans*	3-Chlorophenyl	4-Fluorophenyl	4.4	3.7	194 ± 14	492 ± 99	2.3
15z, *trans*	3-Chlorophenyl	3-Methoxyphenyl	4.3	3.7	789 ± 116	—	1.8
15aa, *trans*	3-Chlorophenyl	4-Methoxyphenyl	4.3	3.7	266 ± 16	674 ± 178	2.3
15ab, *trans*	3-Chlorophenyl	4-Dimethylaminophenyl	4.4	3.5	473 ± 30	—	1.9
15ac, *trans*	3-Chlorophenyl	3-Dimethylaminophenyl	4.4	3.5	>10,000	—	—
15ad, *trans*	3-Chlorophenyl	Pyrazin-2-yl	2.9	5.1	1370 ± 176	—	3.0
15ae, *trans*	3-Chlorophenyl	Pyrimidin-2-yl	2.9	5.1	425 ± 187	3790 ± 467	3.5
15af, *trans*	3-Chlorophenyl	Pyridin-2-ylmethyl	2.5	5.1	>10,000	—	—
15ag, *trans*	3-Chlorophenyl	Cyclohexyl	4.3	3.8	857 ± 73	—	1.7
MPEP	—	—	3.8	3.1	2.3 ± 0.3	3.4 ± 0.5	4.9

[a] Human mGluR5 IC_{50} (FLIPR functional assay[24]) and K_i (binding assay[25]) values are expressed as mean ± S.E.M (nM) of three or four separate experiments except for 15n (FLIPR IC_{50} is the average value of two experiments).
[b] LLE = $pIC_{50} - c\text{Log}P$.
[c] Absolute configurations arbitrarily assigned.
[d] *cis*/*trans* refers to an achiral mixture of cis- and trans-isomers made from **16** (*cis*/*trans* ~3:1).

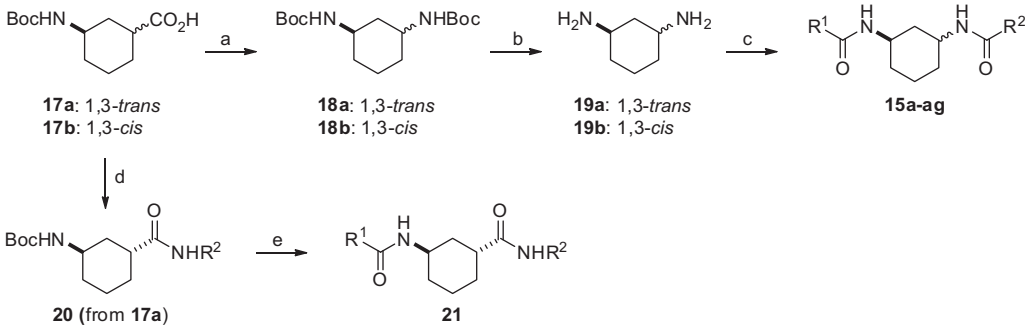

Scheme 2. Synthesis of *trans*- or *cis*-diamides. Reagents and conditions: (a) (i) DPPA (1 equiv), NEt_3 (1 equiv), toluene, reflux, 1 h, (ii) *t*-BuOH (2 equiv), reflux, 12 h, 40–60%; (b) TFA, CH_2Cl_2, room temp, 1 h, 100% conversion, used without purification; (c) (i) NEt_3 (4 equiv), R^1CO_2H (1 equiv), BOP (1 equiv), CH_2Cl_2, room temp, overnight; or NEt_3 (3 equiv), R^1COCl (1 equiv), CH_2Cl_2, 0 °C to room temp 20–45%, (ii) NEt_3 (4 equiv), R^2CO_2H (1 equiv), BOP (1 equiv), CH_2Cl_2, room temp overnight; or NEt_3 (3 equiv), R^2COCl (1 equiv), CH_2Cl_2, 0 °C to room temp; 60–90%; (d) R^2NH_2 (1 equiv), BOP (1 equiv), NEt_3 (2 equiv), CH_2Cl_2, room temp, overnight; ~70%; (e) (i) TFA, CH_2Cl_2, 30 min, (ii) NEt_3 (4 equiv), R^1CO_2H (1 equiv), BOP (1 equiv), CH_2Cl_2, room temp, overnight; ~25–60%.

functional assay (IC_{50} >10,000 nM). This lack of activity may result from a need for a binding interaction with the amide N–H, or may be due to energetically unfavorable conformational changes caused by introduction of a methyl group on the amide moiety.

Select compounds were evaluated in a binding assay (Table 1). The affinities (K_i) of these compounds shifted to the right by 1.5–9 fold compared to IC_{50} values. Racemic mixtures of key compounds **15a**, **15e** and **15u** were resolved by chiral HPLC[28] into the corresponding trans homochiral analogs **15c** and **15d**; **15f** and **15g**; and **15w** and **15x**, respectively. Absolute configurations were assigned arbitrarily. Screening these compounds showed that the mGluR5 NAM activity in this chemotype resides in one

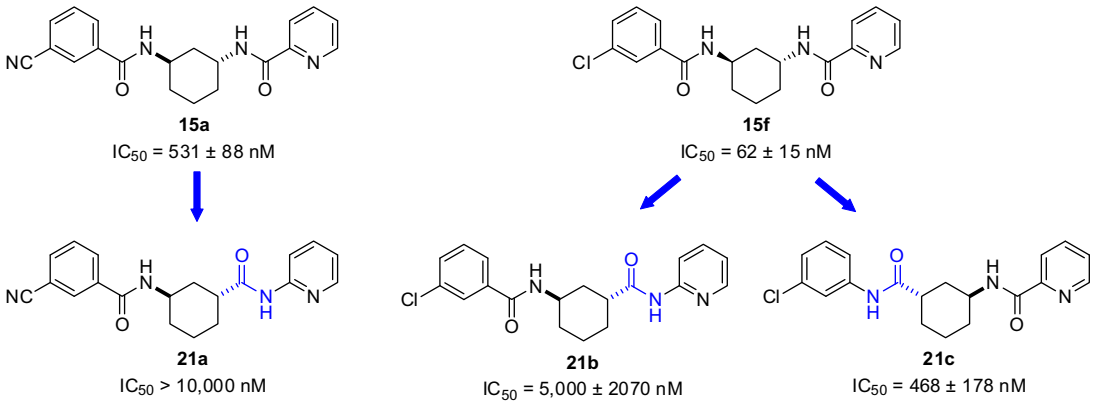

Scheme 3. mGluR5 NAM activity of a set of amides and retroamides.

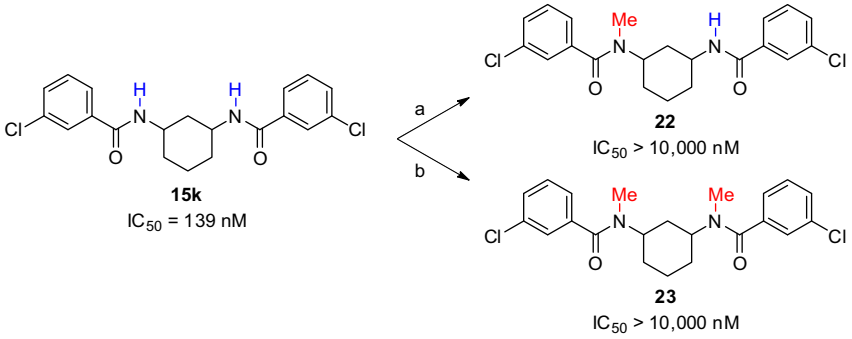

Scheme 4. Reagents and conditions: (a) NaH (2 equiv), MeI (2 equiv), DMF, room temp, 16 h, 3%; (b) NaH (5 equiv), MeI (10 equiv), DMF, room temp, 16 h, 14%.

enantiomer. The three active enantiomers **15c**, **15f** and **15w** were further profiled in a rat mGluR1 functional screen (to explore mGluR Group 1 potential cross-reactivity), human, rat and mouse liver microsomal stability, human plasma protein binding and physicochemical property assays, and the results are summarized in Table 2. Compounds **15w** and **15f** are equipotent in vitro, and have about 4-fold more efficacy than **15c** in the functional screen, and about 6-fold higher affinity than **15c** in the binding assay. All three compounds showed good selectivity against rmGluR1, appropriate plasma free fraction, and their human liver microsomal intrinsic clearances are below human liver hepatic blood flow. Compound **15w** has high Log$D_{7.4}$ (>5) and low aqueous solubility at pH 7.4 (5 μM). Compound **15f** has the best balance of properties among these three compounds. We proceeded to explore brain partition in mouse, as well as rat and mouse brain homogenate free fraction and pharmacokinetic properties (Table 3). In rat, this compound showed high oral bioavailability (F = 0.8), moderate volume distribution (V_{ss} = 3.4 L/kg), high plasma clearance (CLp = 4.1 L/h/kg, 85% of rat hepatic blood flow) and short half life ($T_{1/2}$ = 0.6 h). Plasma and brain free fractions in rodent were high. Upon sc dosing in mouse at a 10 mg/kg dose, CNS penetration was deemed appropriate, with brain to plasma concentrations ratio (B/P) of 0.34 and unbound brain to unbound plasma concentrations ratio (Kupp) of 0.67 1 h post-dosing. However, the free brain concentration in mouse at this dose and time point (170 nM × 0.22 = 37 nM) only covered a fraction of K_i due to suboptimal affinity (K_i = 205 nM). We deemed further gains in affinity and functional potency were required.

We set to explore whether the affinity at mGluR5 could be improved by constraining the conformation of one of the amide bonds in **15**. Among a number of options conceived, a spirooxazoline template (Fig. 3) was designed and found to satisfy the binding hypothesis using our computational overlay model. Compounds **24a**–**i** were made according to Scheme 5. Their in silico properties and in vitro mGluR5 activities are shown in Table 4. For these constrained analogs, the binding affinities (K_i) are comparable to their IC_{50} values. Unlike the diamide template, where a methyl at 6-position of pyridyl has no significant impact on affinity and functional potency (**15p** (racemate) vs. des-methyl analog **15f** (chiral)), a methyl at 6-position of the pyridyl in the spirooxazoline template enhances the affinity and potency by about 5-fold (**24d** vs. **24g**); pyridin-3-yl and pyridin-4-yl analogs in the diamide template are active (**15n** and **15o**, IC_{50} <650 nM), while the corresponding analogs in the spirooxazoline template are inactive at highest

Table 2
Properties of active homochiral analogs

CMPD	rmGluR1[29]		Liver microsomal CL_{int}[30,a]			Human PPB%[31]	Solubility[32] (μM)	Log$D_{7.4}$[33]
	EC_{50} (nM)	IC_{50} (nM)	Human (L/min)	Rat (mL/min)	Mouse (mL/min)			
15c	>10,000	>10,000	0.5	8.3	1.8	84.3	240	–
15f	>10,000	>10,000	1.1	41	9	93.5	240	3.2
15w	>10,000	2100	0.8	9.4	nd	96.1	5.4	>5

[a] Human hepatic blood flow = 1.5 L/min; rat hepatic blood flow = 20 mL/min; mouse hepatic blood flow = 1.8 mL/min.

Table 3
Brain homogenate free fraction and in vivo PK of compound **15f**

Rat free fraction%[31]		Mouse free fraction%[31]		Exposure in mouse[a]				In vivo rat PK[b]						
B	P	B	P	B (nM)	P (nM)	B/P	Kupp	C_{max} (ng/mL)	T_{max} (h)	CLp (L/h/kg)	V_{ss} (L/kg)	$T_{1/2}$ (h)	$AUC_{0\text{-}inf}$ (ng.h/mL)	F
13	14	22	11	170	500	0.34	0.67	220	2	4.1	3.4	0.6	260 (IV) 530 (PO)	0.8

[a] Brain (B) and plasma (P) exposures determined at 1 h following 10 mg/kg, SC in CD-1 mice ($n = 2$) using 20% hydroxypropyl-β-cyclodextrin in water as dosing vehicle. Average values ($n = 2$) are given. Limit of quantification was 2 ng/g and 2 ng/mL for brain homogenate and plasma, respectively.
[b] The study was performed in SD rats ($n = 2$) in a cross-over manner with 24 h washout period. IV: 1 mg/kg; PO: 2 mg/kg; vehicle: 20% hydroxypropyl-β-cyclodextrin in water.

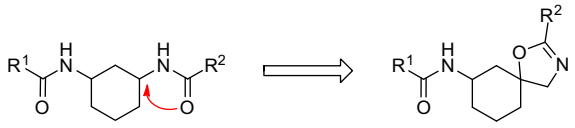

Figure 3. Design of spirooxazoline.

testing concentration (10 μM), indicating differences in SAR between the two chemotypes. Compounds **24d** and **24g** were further profiled for their selectivity against mGluR1, in vitro metabolic stability, exposure in rodent and free brain fraction (Table 5). Both compounds are highly selective against mGluR1, have high liver microsomal intrinsic clearance, good CNS penetration, and high plasma and brain exposure in mouse 1 h after sc dosing. Compound **24d** was also evaluated in a mouse marble burying test[35] and demonstrated anxiolytic-like activity determined 1 h after sc administration of a single 30 mg/kg dose (Fig. 4). In the absence of exposure from this study, an extrapolated free brain concentration at 30 mg/kg based on an exposure study at 10 mg/kg, 1 h would be 3 nM, which is lower than K_i (30 nM). However, actual exposures may be higher due to combination of potentially nonlinear pharmacokinetics from 10 to 30 mg/kg and experimental errors between the two studies. Since both compounds have

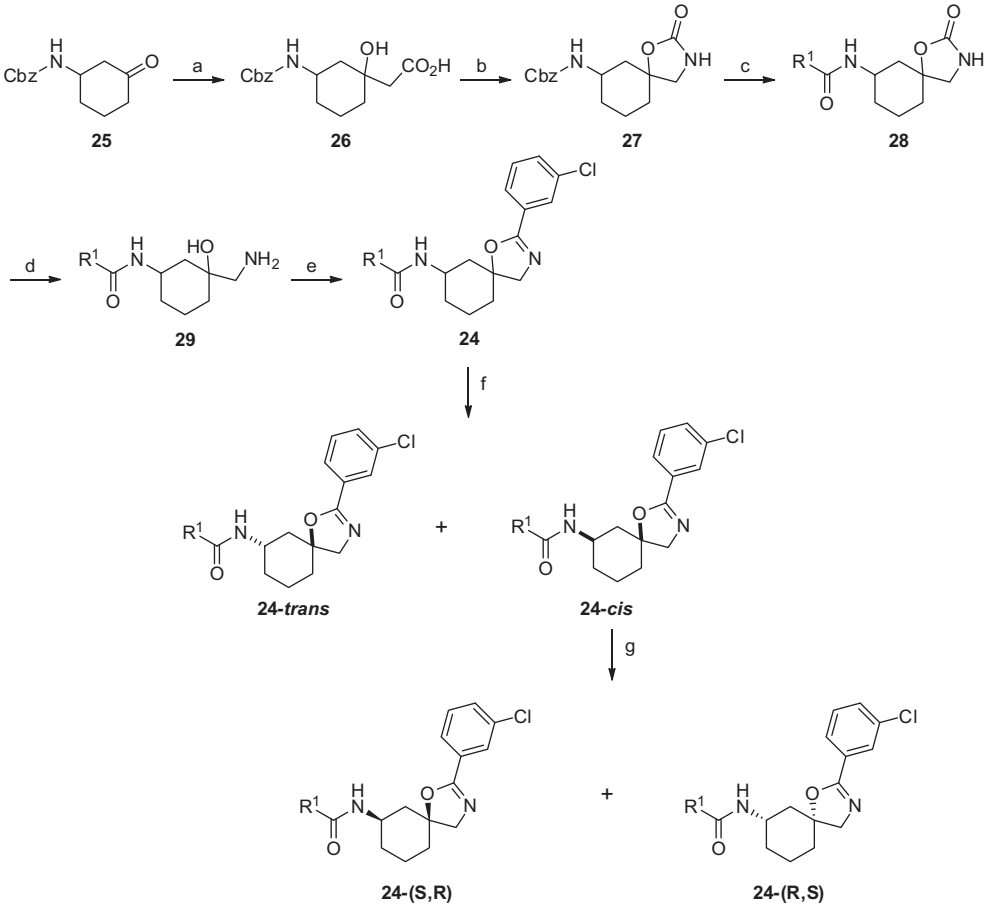

Scheme 5. Reagents and conditions: (a) (i) LHMDS (1.1 equiv), THF, EtOAc (1.1 equiv) −78 °C; (ii) LiOH·H_2O (10 equiv), THF/H_2O (1:1), rt, overnight; two-step crude yield 75%; (b) DPPA (1 equiv), toluene, TEA (1 equiv), rt, 30 min, then reflux, 8 h, 74%; (c) (i) Pd/C, MeOH, H_2, 50 psi, 4 h, crude yield 95%; (ii) R^1CO_2H (1 equiv), TEA (4 equiv), BOP (1 equiv), DCM; ~70%; (d) LiOH·H_2O (10 equiv), dioxane/H_2O (1:1), 70 °C, 5 h, crude yield 85%; (e) 3-chloro-benzimidic acid ethyl ester (1.5 equiv), EtOH, 1 drop 4 M HCl in dioxane, 100 °C, microwave, 20–30 min, ~60%; (f) silica gel chromatography (hexane/ethyl acetate); less polar fraction assigned as *trans* and more polar fraction assigned *cis*; (g) resolution by chiral HPLC: Chiralpak AD (Diacel), 250 × 20 mm; mobile phase: 20% isopropanol, 79.9% hexane, 0.1% diethylamine; flow rate: 14 mL/min; UV at 254 nM; front peak arbitrarily assigned as (*S*,*R*) and back peak arbitrarily assigned as (*R*,*S*). *Cis* assignment (as defined above) was based on the NMR spectroscopy analyses (COSY, ROESY, edited HSQC overlaid with HMBC) of compound **24d**.[34]

Table 4
In vitro mGluR5 activity and in silico properties of cyclohexyl spirooxazolines

CMPD	R[1]	*c*Log *P*	MPO	IC_{50}[a] (nM)	*Ki*[a] (nM)	LLE[b]
24a, *trans*	6-Methylpyridin-2-yl	4.8	3.8	1505	—	1.0
24b-, *cis*				72	—	2.4
24c, *cis*-(*S*,*R*)				5225	—	0.5
24d, *cis*-(*R*,*S*)				23	30 ± 4	2.9
24e, *cis*/*trans* mixture	Pyridin-2-yl	4.3	4.1	647	—	1.9
24f, *cis*-(*S*,*R*)				2910	—	1.3
24g, *cis*-(*R*,*S*)				115	178 ± 3	2.7
24h, *cis*/*trans* mixture	Pyridin-3-yl	3.9	4.3	>10,000	—	—
24i, *cis*/*trans* mixture	Pyridin-4-yl	3.9	4.3	>10,000	—	—

[a,b] Same as described in Table 1.

Table 5
mGluR1 selectivity and DMPK profile of compounds **24d** and **24g**

CMPD	rmGluR1[29] EC_{50} (IC_{50}) (nM)	Liver microsomal CL_{int}[30]			Mouse free fraction%[31]		Exposure in rodent at 10 mpk, 1 h[a]						
							Rat, PO			Mouse			
		Human (L/min)	Rat (mL/min)	Mouse (mL/min)	B	P	B (nM)	P (nM)	B/P	B (nM)	P (nM)	B/P	Kupp
24d	>10,000 (>10,000)	13	48	12.5	0.3	0.2	ND	ND	ND	PO: 9 SC: 910	PO: 17 SC: 1175	0.5 0.8	PO: 0.8 SC: 1.1
24g	>10,000 (>10,000)	13	160	8.8	0.5	0.3	5	8	0.6	SC: 1165	SC: 1165	1.0	SC: 1.6

[a] Same conditions as described in Table 3.

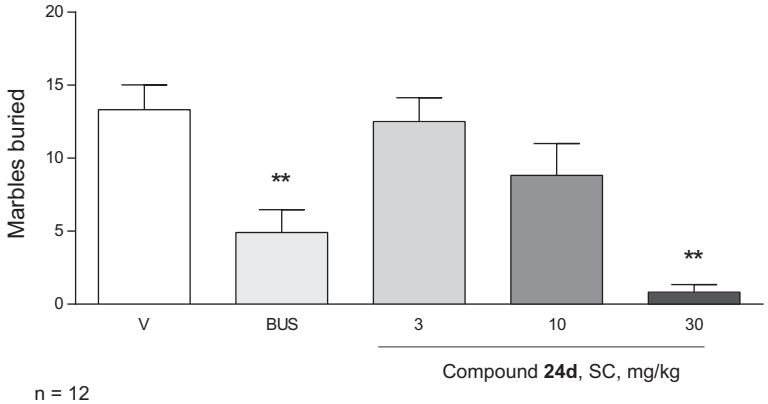

n = 12
V: 20% HPβCD in water, vehicle group
BUS: positive control group treated with buspirone (10 mg/kg, free base in distilled water, SC)
Treatment time: 30 min ** P< 0.01 vs. vehicle group (ANOVA with post-hoc Dunnett's test)

Figure 4. Effect of compound **24d** on marble burying in male CD-1 mice.

extremely low oral exposure, a chemical stability test of compound **24g** under acidic conditions was performed.[36] More than 50% of the compound was missing after incubation in methanol at 37 °C, pH 1.5 for 1 h, forming a single major product with molecular weight 18 amu higher than **24g**, presumably due to hydrolytic opening of the oxazolinyl ring. Therefore, both first-pass metabolism and chemical instability at acidic pH contributed to the low oral exposure of compounds in this chemotype. At this point, the decision was made to deprioritize further work related to compound **24d**, and to not establish its absolute configuration. Instead, resources were directed towards solving the chemotype's instability problems. This led to a novel spirocyclic lactam template, the absolute stereochemistry of which was found to be *R*,*R*.[38] This work will be the focus of future communications.

In summary, using a computational overlay model built based on literature compounds, a series of *trans*-1,3-cyclohexyl-diamides was discovered as negative allosteric modulators of the mGlu5 receptor lacking an alkyne moiety. Compounds in this chemotype are characterized by tractable SAR, reasonable in vitro potency and good brain penetration in rodents. Conformational constraint of one of the amide bonds in the diamide series led to a spirooxazoline template that demonstrated good in vitro mGluR5 activity, high selectivity against mGluR1, good CNS penetration and in vivo efficacy in the mouse marble burying model (representative compound **24d**). The poor oral exposure of compounds in the spirooxazoline template was established as arising from high first-pass metabolism, as well as chemical instability under acidic conditions. Further modifications of these two chemotypes were explored seeking improvements in functional potency, binding affinity, chemical stability and in vivo clearance, which led to a number of non-alkyne chemotypes with enhanced properties.[28,37,38] These will be the topic of future reports.

Acknowledgments

We are grateful to Drs. Mark Hayward, Qing-ping Han, Chi Zhang and Xu Zhang for solubility and Log$D_{7.4}$ determinations, compound purification, and racemic compound resolution, to Xiaosui Pu, Noel J. Boyle and Veena Menon for in vitro pharmacology determinations, to Manuel Cajina, Megan E. Nattini and Kimloan Nguyen for in vitro and in vivo DMPK and bioanalytical support, to Christina Sveigaard for rodent plasma and brain free fractions determination, to Dr. Jens-Jakob Karlsson for coordinating in vitro DMPK studies at a CRO. We acknowledged Dr. Lena Tagmose for her constructive comments to this manuscript.

Supplementary data

Supplementary data associated with this article can be found, in the online version, at http://dx.doi.org/10.1016/j.bmcl.2012.12.078.

Reference and notes

1. Kew, J. N. C.; Kemp, J. A. *Psychopharmacology* **2005**, *179*, 4.
2. Oswald, R. E.; Ahmed, A.; Fenwick, M. K.; Loh, A. P. *Curr. Drug Targets* **2007**, *8*, 573.
3. Recasens, M.; Guiramand, J.; Aimar, R.; Abdulkarim, A.; Barbanel, G. *Curr. Drug Targets* **2007**, *8*, 651.
4. Swanson, C. J.; Bures, M.; Johnson, M. P.; Linden, A. M.; Monn, J. A.; Schoepp, D. D. *Nat. Rev. Drug Disc.* **2005**, *4*, 131.
5. Pin, J. P.; Duvoisin, R. *Neuropharmacology* **1995**, *34*, 1.
6. Conn, P. J.; Pin, J. P. *Annu. Rev. Pharmacol. Toxicol.* **1997**, *37*, 205.
7. Goudet, C.; Vilar, B.; Courtiol, T.; Deltheil, T.; Bessiron, T.; Brabet, I.; Oueslati, N.; Rigault, D.; Bertrand, H. O.; McLean, H.; Daniel, H.; Amalric, M.; Acher, F.; Pin, J. P. *FASEB J.* **2012**, *26*, 1682.
8. Topiol, S.; Sabio, M.; Uberti, M. *Neuropharmacology* **2011**, *60*, 93.
9. Conn, P. J.; Christopoulos, A.; Lindsley, C. W. *Nat. Rev. Drug. Disc.* **2009**, *8*, 41.
10. O'Neill, M. J.; Fell, M. J.; Svensson, K. A.; Witkin, J. M.; Mitchell, S. N. *Drugs Future* **2010**, *35*, 307.
11. Nicoletti, F.; Bockaert, J.; Collingridge, G. L.; Conn, P. J.; Ferraguti, F.; Schoepp, D. D.; Wroblewski, J. T.; Pin, J. P. *Neuropharmacology* **2011**, *60*, 1017.
12. Rocher, J. P.; Bonnet, B.; Bolea, C.; Lutjens, R.; Le Poul, E.; Poli, S.; Epping-Jordan, M.; Bessis, A. S.; Ludwig, B.; Mutel, V. *Curr. Top. Med. Chem.* **2011**, *11*, 680.
13. Jacquemont, S.; Curie, A.; des Portes, V.; Torrioli, M. G.; Berry-Kravis, E.; Hagerman, R. J.; Ramos, F. J.; Cornish, K.; He, Y.; Paulding, C.; Neri, G.; Chen, F.; Hadjikhani, N.; Martinet, D.; Meyer, J.; Beckmann, J. S.; Delange, K.; Brun, A.; Bussy, G.; Gasparini, F.; Hilse, T.; Floesser, A.; Branson, J.; Bilbe, G.; Johns, D.; Gomez-Mancilla, B. *Sci. Transl. Med.* **2011**, *3*, 64.
14. Berg, D.; Godau, J.; Trenkwalder, C.; Eggert, K.; Csoti, I.; Storch, A.; Huber, H.; Morelli-Canelo, M.; Stamelou, M.; Ries, V.; Wolz, M.; Schneider, C.; Di Paolo, T.; Gasparini, F.; Hariry, S.; Vandemeulebroecke, M.; Abi-Saab, W.; Cooke, K.; Johns, D.; Gomez-Mancilla, B. *Mov. Disord.* **2011**, *26*, 1243.
15. Zerbib, F.; Bruley des Varannes, S.; Roman, S.; Tutuian, R.; Galmiche, J.-P.; Mion, F.; Tack, J.; Malfertheiner, P.; Keywood, C. *Aliment. Pharmacol. Ther.* **2011**, *33*, 911.
16. Pecknold, J. C.; McClure, D. J.; Appeltauer, L.; Wrzesinski, L.; Allan, T. J. *Clin. Psychopharmacol.* **1982**, *2*, 129.
17. Development of ADX10059 Ended for Long-term Use. http://www.addexpharma.com/press-releases-details/article/development-of-adx10059-ended-for-long-term-use/ (accessed October 2010).
18. (a) Raboisson, P.; Breitholtz-Emanuelsson, A.; Dahlloef, H.; Edwards, L.; Heaton, W. L.; Isaac, M.; Jarvie, K.; Kers, A.; Minidis, A. B. E.; Nordmark, A.; Sheehan, S. M.; Slassi, A.; Stroem, P.; Terelius, Y.; Wensbo, D.; Wilson, J. M.; Xin, T.; McLeod, D. A. *Bioorg. Med. Chem. Lett.* **2012**, *22*, 6974; (b) Plitt, P.; Hauptmeier, B.; Boderke, P. PCT Int. Appl. WO 2011064237, 2011.; (c) Bertinato, P.; Fichman, M.; Ghosh, S.; Lin, J.; Segal, D.; Zhang, Z. PCT Int. Appl. WO 2010049366, 2010.; (d) Wagner, G.; Weber, C.; Nyeki, O.; Nogradi, K.; Bielik, A.; Molnar, L.; Bobok, A.; Horvath, A.; Kiss, B.; Kolok, S.; Nagy, J.; Kurko, D.; Gal, K.; Greiner, I.; Szombathelyi, Z.; Keseru, G. M.; Domany, G. *Bioorg. Med. Chem. Lett.* **2010**, *20*, 3737; (e) Mueller, R.; Dawson, E. S.; Meiler, J.; Rodriguez, A. L.; Chauder, B. A.; Bates, B. S.; Felts, A. S.; Lamb, J. P.; Menon, U. N.; Jadhav, S. B.; Kane, A. S.; Jones, C. K.; Gregory, K. J.; Niswender, C. M.; Conn, P. J.; Olsen, C. M.; Winder, D. G.; Emmitte, K. A.; Lindsley, C. W. *ChemMedChem* **2012**, *7*, 406; (f) Weiss, J. M.; Jimenez, H. N.; Li, G.; April, M.; Uberti, M. A.; Bacolod, M. D.; Brodbeck, R. M.; Doller, D. *Med. Chem. Lett.* **2011**, *21*, 4891; (g) Emmitte, K. A. *ACS Chem. Neurosci.* **2011**, *2*, 41.
19. Topiol, S. W.; Li, G.; Zhou, H.; Jimenez, H.; Doller, D. in preparation.
20. (a) Edwards, L.; Isaac, M.; Slassi, A.; Sun, G.; Xin, T.; Minidis, A.; Dove, P. U.S. Pat. Appl. Publ. US 20070037816, 2007.; (b) Edwards, L.; Isaac, M.; Slassi, A.; Sun, G.; Dove, P.; Arzel, E. U.S. Pat. Appl. Publ. US 20070037817, 2007.
21. MOE; Chemical Computing Group: Montreal, Quebec, Canada, 2009.
22. Wager, T. T.; Hou, X.; Verhoest, P. R.; Villalobos, A. *ACS Chem. Neurosci.* **2010**, *1*, 435.
23. A mixture of cyclohexane-1,3-diamine (50 mg, 0.44 mmol), picolinic acid (54 mg, 0.44 mmol), TEA (0.24 mL, 1.76 mmol) and BOP (194 mg, 0.44 mmol) in DCM (2 mL) was stirred at rt overnight. To the reaction mixture was added 3-cyanobenzoic acid (65 mg, 0.44 mmol), (0.24 mL, 1.76 mmol) and BOP (194 mg, 0.44 mmol). After stirring at rt overnight, the reaction mixture was diluted with DCM, washed with ½ saturated $NaHCO_3$ and brine, dried over Na_2SO_4, and concentrated under reduced pressure. The residue was purified on a preparative TLC plate (hexane/ethyl acetate: 1/1). ^{1}H NMR and HSQC indicated that the compound less polar on the TLC plate was *trans* (**15a**) and the compound more polar on the TLC plate was *cis* (**15b**), where the ^{1}H NMR signals for the CH_2-groups in the cyclohexane ring showed characteristic patterns. For **15b**, the protons were clearly axial/equatorial pairs with large differences in chemical shifts in accordance with a chair conformation which is preferred with the cis-configuration. This could be seen unambiguously for CH_2's in position 2 and 5 from the standard HSQC spectrum and allowed the assignment: H-2_{ax} 1.37 ppm, quartet, J = 11.7 Hz; H-2_{eq} 2.50 ppm, br d; H-5_{ax} 1.60, multiplet; H-5 equiv 1.93 ppm, multiplet. For **15a**, the chemical shift of the protons within the same CH_2-groups are almost identical in agreement with a boat/twist boat conformation, which would be expected for the trans-configuration. **15a**: ^{1}H NMR (500.13 MHz, $CHCl_3$-*d*) δ 8.57 (d, J = 4.5 Hz, 1H), 8.21 (d, J = 7.5 Hz, 1H), 8.16 (d, J = 7.8 Hz, 1H), 8.08 (s, 1H), 8.00 (d, J = 7.8 Hz, 1H), 7.85 (dt, J = 7.8 Hz, 1.9 Hz, 1H), 7.78 (d, J = 7.8 Hz, 1H), 7.57 (t, J = 7.8 Hz, 1H), 7.44 (ddd, J = 7.8 Hz, 4.5 Hz, 1.9 Hz, 1H), 6.34 (d, J = 6.7 Hz, 1H), 4.33–4.45 (m, 2H), 1.86–2.05 (m, 4H), 1.60–1.86 (m, 4H). **15b:** ^{1}H NMR (500.13 MHz, $CHCl_3$-*d*) δ 8.53 (d, J = 4.6 Hz, 1H), 8.20 (d, J = 7.8 Hz, 1H), 8.02 (s, 1H), 7.99 (d, J = 7.8 Hz, 1H), 7.85 (dt, J = 7.8 Hz, 1.6 Hz, 1H), 7.77 (d, J = 7.8 Hz, 1H), 7.56 (t, J = 7.8 Hz, 1H), 7.44 (dd, J = 7.8 Hz, 4.6 Hz, 1H), 6.00 (d, J = 7.3 Hz, 1H), 4.06–4.19 (m, 2H), 2.50 (br d, 1H), 2.09 (m, 2H). 1.89–1.96 (m, 1H), 1.53–1.64 (m, 1H), 1.37 (q, J = 11.7 Hz, 1H), 1.19–1.33 (m, 2H).
24. Human mGluR5 FLIPR assay: The cDNA for human metabotropic glutamate receptor 5 was a generous gift from S. Nakanishi (Kyoto University, Kyoto, Japan). The hmGluR5 was stably expressed in a HEK 293 cell line and grown in Dulbecco's Modified Eagle Medium (DMEM) (Invitrogen, Carlsbad, CA) with supplements (10% bovine calf serum, 4 mM glutamine, 100 units/mL penicillin, 100lg/mL streptomycin and 0.75 mM G1418) at 37 °C, 5% CO_2. Twenty-four hours prior to assay, cells were seeded into 384-well black wall microtiter plates coated with poly-D-lysine. Just prior to assay, media was aspirated and cells dye-loaded (25 μL/well) with 3 μM 20 Fluo-4/0.01% pluronic acid in assay buffer (Hank's Balanced Saline Solution (HBSS)): 150 mM NaCl, 5 mM KCl, 1 mM $CaCl_2$, 1 mM $MgCl_2$, plus 20 mM *N*-2-hydroxyethylpiperazine-*N*′-2-ethanesulfonic acid (HEPES), pH 7.4, 0.1% bovine serum albumin (BSA) and 2.5 mM probenecid) for 1 h in 5% CO_2 at 37 °C. After excess dye was discarded, cells were washed in assay buffer and layered with a final volume equal to 25 μL/well. Basal fluorescence is monitored in a fluorometric imaging plate reader (FLIPR, Molecular Devices, Sunnyvale, CA) with an excitation wavelength of 488 nM and an emission range of 500–560 nM. Laser excitation energy was adjusted so that basal fluorescence readings were approximately 10,000 relative fluorescent units. Cells were stimulated with an EC_{20} or an EC_{80} concentration of glutamate in the presence of a compound to be tested, both diluted in assay buffer, and relative fluorescent units were measured at defined intervals (exposure = 0.6 s) over a 3 min period at room temperature. Basal readings derived from negative controls were subtracted from all samples. Maximum change in fluorescence was calculated for each well. Concentration–response curves derived from the maximum change in fluorescence were analyzed by nonlinear regression (Hill equation). An antagonist can be identified from these concentration–response curves if a compound produces a concentration dependent inhibition of the EC_{80} glutamate response.
25. Binding assays were performed described in [O'Brien, J. A. et al. *Mol. Pharmacol.* **2003**, *64*, 731] with slight modifications. Briefly, after thawing, the membrane homogenates were resuspended in 50 mM Tris–HCl, 0.9% NaCl binding buffer at pH 7.4 to a final assay concentration of 40 μg protein/well for [^{3}H] 1,3-((6-methylpyridin-2-yl)ethynyl)cyclohex-2-enone *O*-methyl oxime ([^{3}H] ABP-688, American Radiolabeled Chemicals, Inc., St. Louis, MO) filtration binding. Incubations included 5 nM [^{3}H]-ABP 688, membranes and either buffer or varying concentrations of compound. Samples were incubated for 60 min at room temperature with shaking. Non-specific binding was defined with 10 μM of RO4917523 (compound **2** in Fig. 1). After incubation, samples were filtered over a GF/C filter (presoaked in 0.25% polyethyleneimine (PEI)) and then washed four time using a Tomtec® Harvester 96® Mach III cell harvester (Tomtec, Hamden, CT) with 0.5 mL ice-cold 50 mM Tris–HCl (pH 7.4). IC_{50} values were derived from the inhibition curve and K_i values were calculated according to the Cheng and Prusoff equation of $K_i = IC_{50}/(1 + [L]/K_d)$ described in [Cheng, Y.; Prusoff, W. H. *Biochem. Pharmacol.* **1973**, *22*, 3099] where [*L*] is the concentration of radioligand and K_d is its dissociation constant at the receptor, derived from the saturation isotherm.
26. Ghosh, A. K.; McKee, S. P.; Thompson, W. J.; Darke, P. L.; Zugay, J. C. *J. Org. Chem.* **1993**, *58*, 1025.
27. Li, G.; April, M.; Austin, J.; Zhou, H.; Pu, X.; Boyle, N. J.; Uberti, M. A.; Brodbeck, R. M.; Bacolod, M. D.; Smith, D. G.; Doller, D. *Neuropharmacology* **2011**, *9*, 35.
28. Column: Chiralpak® AD(Daicel), 250 × 20 mm. Mobile phase: 20% isopropanol, 79.9% hexane, 0.1% diethylamine. Flow rate: 14 mL/min. UV detector: 254 nM.
29. Rat mGluR1 FLIPR assay: The cDNA for rat metabotropic glutamate receptor 1 was a generous gift from S. Nakanishi (Kyoto University, Kyoto, Japan). The

rmGluR1 was stably expressed in a HEK 293 cell line and grown in Dulbecco's Modified Eagle Medium (DMEM) (Invitrogen, Carlsbad, CA) with supplements (1.5% bovine calf serum, 4 mM glutamine, 100 units/mL penicillin, 100l g/mL streptomycin and 0.75 mM G1418) at 37 °C, 5% CO_2. Twenty-four hours prior to assay, cells were seeded into 384-well black wall microtiter plates coated with poly-D-lysine. Just prior to assay, media was aspirated and cells dye-loaded (25 μL/well) with 3 μM 20 Fluo-4/0.01% pluronic acid in assay buffer (Hank's Balanced Saline Solution (HBSS)): 150 mM NaCl, 5 mM KCl, 1 mM $CaCl_2$, 1 mM $MgCl_2$, plus 20 mM *N*-2-hydroxyethylpiperazine-*N*'-2-ethanesulfonic acid (HEPES), pH 7.4, 0.1% bovine serum albumin (BSA) and 2.5 mM probenecid) for 1 h in 5% CO_2 at 37 °C. After excess dye was discarded, cells were washed in assay buffer and layered with a final volume equal to 25 μL/well. Basal fluorescence is monitored in a fluorometric imaging plate reader (FLIPR, Molecular Devices, Sunnyvale, CA) with an excitation wavelength of 488 nM and an emission range of 500–560 nM. Laser excitation energy was adjusted so that basal fluorescence readings were approximately 10,000 relative fluorescent units. Cells were stimulated with an EC_{20} or an EC_{80} concentration of glutamate in the presence of a compound to be tested, both diluted in assay buffer, and relative fluorescent units were measured at defined intervals (exposure = 0.6 s) over a 3 min period at room temperature. Basal readings derived from negative controls were subtracted from all samples. Maximum change in fluorescence was calculated for each well. Concentration–response curves derived from the maximum change in fluorescence were analyzed by nonlinear regression (Hill equation).

30. Determination of metabolic stability in liver microsomes: This study was conducted by incubating 1 μM concentration of test compounds at 37 °C in pooled male rat or pooled human liver microsomes (0.5 mg/mL) in 0.1 M potassium phosphate buffer (pH 7.4) supplemented with NADPH-regenerating system (1.3 mM $NADP^+$, 3 mM $MgCl_2$, 3.5 mM glucose-6-phosphate, and 4 units glucose-6-phosphate dehydrogenase). Aliquots were taken at 0.25, 5, 15, 30 and 60-minute time points. The aliquots were added to a 96-well plate containing an equal volume of acetonitrile in order to terminate the reaction. The samples were vortexed and centrifuged at 3000 rpm for 15 min. A known volume of internal standard was added to the supernatant. The samples were injected in an LC–MS/MS system to monitor the disappearance of the parent compound. The half-life was measured by plotting the log of the remaining compound versus time. The in vitro half-life data were used to calculate the intrinsic clearance (CL_{int}), according to the equation shown below:

$$CL_{int} = 0.693 \times \frac{1}{T_{1/2}(\text{min})} \times \frac{g \text{ liver weight}}{kg \text{ body weight}} \times \frac{mL \text{ incubation}}{mg \text{ microsomal protein}} \times \frac{mg \text{ microsomal protein}}{g \text{ liver weight}} \times kg \text{ body weight}$$

where, liver weight is 20 g/kg in human and 45 g/kg in rat, and body weight is 70 kg for human and 250 g in rat. In this equation, it was assumed that 1 g of liver contains 45 mg of microsomal protein and the binding of the drug to microsomal proteins was assumed to be zero, hence the unbound drug fraction, $f_{u,mic} = 1$.

31. Human and rat protein binding, and rat brain homogenate free fraction were determined by using a 96-well format equilibrium dialyzer (HTD96b, Catalog# 1006, http://www.htdialysis.com). Test compounds (10 μM) were spiked into serum from human or rat, or rat brain homogenate, and dialyzed against phosphate buffered saline (pH 7.4) via a >5000 molecular weight dialysis membrane for 2.5 h in an incubator set to maintain 37 °C with 5% CO_2. The dialysis block was placed on an orbital shake. After 2.5 h incubation, buffer and serum samples (or brain homogenate samples) were collected and transferred into a 96-well matrix plate with tube inserts. Internal standards were added and the samples were vortexed and mixed, and analyzed by LC–MS/MS.
32. Kinetic solubility was measured from 10 mM DMSO stock solution of the test compound (300 μL) diluted with 2 × 200 μL of 25 mM potassium phosphate buffer in a Titer plate shaker at a speed of 1.8 for 4 h. The supernatant was analyzed by using a Waters Acquity UPLC system (Column:Acquity UPLC BEH C-18, 1.7 μm 2.1 × 50 mm column and PDA detector at 254 nM for quantitation) with a gradient (mobile phase A: 2% w/v ammonium formate and 20% acetonitrile in water, mobile phase B: 100% acetonitrile) for 2 min.
33. Log*D* at pH 7.4 was determined with solid sample using classic shake flask method described in Gulyaeva, N.; Zaslavsky, A.; Lechner, P.; Chlenov, M.; Chait, A.; Zaslavsky, B. *Eur. J. Pharm. Sci.* **2002**, *17*, 81.
34. NMR analysis of compound **24d**: From the standard HSQC and COSY spectra **24d** proton 7 (CH, 4.10 ppm, br s) and protons 4 (CH_2, AB-system, 3.77 ppm (d, *J* = 14.9 Hz) and 3.81 ppm (d, *J* = 14.9 Hz) could be assigned. In the 2D-ROESY spectrum the 4 and 7 protons show a distance correlation. This can only be true in the case of cis-configuration with the spiro-6-ring in a chair conformation with oxygen 1 and amide-N in an equatorial position. ^{1}H NMR (600.13 MHz, DMSO-d_6) δ 8.66 (d, *J* = 8.3 Hz, 1H), 7.87 (t, *J* = 7.5 Hz, 1H), 7.8–7.86 (m, ^{3}H), 7.63 (ddd, *J* = 7.9 Hz, 2.2 Hz, 0.9 Hz, 1H), 7.50 (t, *J* = 7.9 Hz, 1H), 7.47 (d, *J* = 7.5 Hz, 1H), 4.1 (br s, 1H), 3.81 (d, *J* = 14.9 Hz, 1H), 3.77 (d, *J* = 14.9 Hz, 1H), 2.53 (s, ^{3}H), 2.03 (d, *J* = 6.0 Hz, 2H), 1.68–1.86 (m, 4H), 1.58–1.68 (m, 1H), 1.45–1.54 (m, 1H). Spectra are in Supplemental.
35. Mouse marble burying:
    (1)Test subjects: Male CD1 mice were obtained from Charles River Laboratories (Kingston, NY), and weighed 25–30 g. Animals were group-housed in a standard colony room with a 12:12 light/dark cycle (lights on at 6:00 am) for at least one week prior to testing. Food and water were provided ad libitum. Animals were weighed, tail marked, and randomly assigned to treatment groups before testing.
    (2) Apparatus: Standard mouse home cages were used as test cages. These cages were individually filled with 1.5 in of Aspen bedding (PWI brand). The bedding was flattened down and two parallel rows of 10 marbles (20 marbles per test cage total) were placed on opposite sides of each cage. Filter tops were used to cover each test cage.
    (3) Treatment: Animals were treated with compound **24d** (3, 10 and 30 mg/kg, dissolved in 20% HPβCD), buspirone (positive control, free base, 10 mg/kg, dissolved in distilled water) and vehicle (20% HPβCD). All animals were dosed subcutaneously with an injection volume of 5 mL/kg.
    (4) Testing procedure: Mice were individually placed in the test cages for a session lasting 30 min after which they were removed and returned to their home cages. The number of fully visible marbles (less than 2/3 covered with bedding) were counted and subtracted from 20 to arrive at the number of marbles buried. Twelve mice were tested per each group.
    (5) Data Analysis: Data were analyzed using One-Way ANOVA with post-hoc Dunnett's test.
36. Chemical stability study: A solution of 0.5 mg of compound **24g** in MeOH (1 mL) and aq HCl (1 mL) at pH 1.5 was shacked at 37 °C for 1 h. The solution was then analyzed by HPLC/MS.
37. Jimenez, H. N.; Li, G.; Doller, D.; Grenon, M.; White, A. D.; Guo, M.; Ma, G. US 7947680.
38. Zhou, H.; Li, G.; Doller, D.; Ma, G. U.S. Pat. Appl. Publ. US 20110098299, 2011.